Replication of optical microlens arrays using photoresist coated molds

Chakrabarti, Maumita; Dam-Hansen, Carsten; Stubager, Jørgen; Pedersen, T. F.; Pedersen, Henrik Chresten

Published in:
Optics Express

Link to article, DOI:
10.1364/OE.24.009528

Publication date:
2016

Document Version
Publisher's PDF, also known as Version of record

Replication of optical microlens array using photoresist coated molds

M. Chakrabarti,[1,*] C. Dam-Hansen,[1] J. Stubager,[1] T. F. Pedersen,[2] and H. C. Pedersen[1]

[1]*DTU Fotonik, Department of Photonics Engineering, Technical University of Denmark, 4000 Roskilde, Denmark*
[2]*Force Technology, Park Allé 345, 2605 Brøndby, Denmark*
**macha@fotonik.dtu.dk*

Abstract: A cost reduced method of producing injection molding tools is reported and demonstrated for the fabrication of optical microlens arrays. A standard computer-numerical-control (CNC) milling machine was used to make a rough mold in steel. Surface treatment of the steel mold by spray coating with photoresist is used to smooth the mold surface providing good optical quality. The tool and process are demonstrated for the fabrication of an ø50 mm beam homogenizer for a color mixing LED light engine. The acceptance angle of the microlens array is optimized, in order to maximize the optical efficiency from the light engine. Polymer injection molded microlens arrays were produced from both the rough and coated molds and have been characterized for lenslet parameters, surface quality, light scattering, and acceptance angle. The surface roughness (R_a) is improved approximately by a factor of two after the coating process and the light scattering is reduced so that the molded microlens array can be used for the color mixing application. The measured accepted angle of the microlens array is 40° which is in agreement with simulations.

OCIS codes: (180.1790) Confocal microscopy; (180.3170) Interference microscopy; (220.3620) Lens system design; (220.4000) Microstructure fabrication; (220.4610) Optical Fabrication; (220.4298) Nonimaging optics; (230.3670) Light-emitting diodes; (240.5450) Polishing; (240.5770) Roughness.

References and links

1. T. J. Suleski and R. D. Te Kolste, "Fabrication trends for free-space microoptics," J. Lightwave Technol. **23**(2), 633–646 (2005).
2. S. Möller and S. R. Forrest, "Improved light out-coupling in organic light emitting diodes employing ordered microlens arrays," J. Appl. Phys. **91**(5), 3324–3327 (2002).
3. S. Park, Y. Jeong, J. Kim, K. Choi, H. C. Kim, D. S. Chung, and K. Chun, "Fabricaton of poly(dimethylsiloxane) microlens for laser-induced fluorescence detection," Jpn. J. Appl. Phys. **45**(6B), 5614–5617 (2006).
4. E. Roy, B. Voisin, J. F. Gravel, R. Peytavi, D. Boudreau, and T. Veres, "Microlens array fabrication by enhanced thermal reflow process: towards efficient collection of fluorescence light from microarrays," Microelectron. Eng. **86**(11), 2255–2261 (2009).
5. P. Schreiber, S. Kudaev, P. Dannberg, and U. D. Zeitner, "Homogeneous LED-illumination using microlens arrays," Proc. SPIE **5942**, 59420K, 59420K-9 (2005).
6. H. C. Pedersen, T. Brockmann, and C. Dam-Hansen, "Light engine for an illumination device," EP2843301, International Bureau of the World Intellectual Property Organization (WIPO) (2015).
7. M. Chakrabarti, A. Thorseth, J. Jepsen, D. D. Corell, and C. Dam-Hansen, "Color control for tunable white LED lighting system," Opt. Eng. in press.
8. M. Chakrabarti, H. C. Pedersen, P. B. Poulsen, and C. Dam-Hansen, "C., "Focusable, color tunable white and efficient LED stage lighting," Opt. Eng. in press.
9. D. Daly, R. F. Stevens, M. C. Hutley, and N. Davies, "The manufacture of microlenses by melting photoresist," Meas. Sci. Technol. **1**(8), 759–766 (1990).
10. K. Naessens, H. Ottevaere, R. Baets, P. Van Daele, and H. Thienpont, "Direct writing of microlenses in polycarbonate with excimer laser ablation," Appl. Opt. **42**(31), 6349–6359 (2003).
11. J. Yong, F. Chen, Q. Yang, G. Du, H. Bian, D. Zhang, J. Si, F. Yun, and X. Hou, "Rapid fabrication of large-area concave microlens arrays on PDMS by a femtosecond laser," ACS Appl. Mater. Interfaces **5**(19), 9382–9385 (2013).
12. P. Zhang, G. Londe, J. Sung, E. Johnson, M. Lee, and H. J. Cho, "Microlens fabrication using an etched glass master," Microsyst. Technol. **13**(3–4), 339–342 (2007).
13. J. Rogers, A. Kärkkäinen, T. Tkaczyk, J. Rantala, and M. Descour, "Realization of refractive microoptics

#257628 Received 18 Jan 2016; revised 2 Apr 2016; accepted 11 Apr 2016; published 22 Apr 2016

through grayscale lithographic patterning of photosensitive hybrid glass," Opt. Express **12**(7), 1294–1303 (2004).
14. K. Totsu, K. Fujishiro, S. Tanaka, and M. Esashi, "Fabrication of three-dimensional microstructure using maskless gray-scale lithography," Sens. Actuators A Phys. **130–131**, 387–392 (2006).
15. B. K. Lee, D. S. Kim, and T. H. Kwon, "Replication of microlens arrays by injection molding," Microsyst. Technol. **10**(6–7), 531–535 (2004).
16. V. N. Goral, Y.-C. Hsieh, O. N. Petzold, R. A. Faris, and P. K. Yuen, "Hot embossing of plastic microfluidic devices using poly(dimethylsiloxane) molds," J. Micromech. Microeng. **21**(1), 017002 (2011).
17. R. K. Jena, C. Y. Yue, Y. C. Lam, P. S. Tang, and A. Gupta, "Comparison of different molds (epoxy, polymer and silicon) for microfabrication by hot embossing technique," Sens. Actuators B Chem. **163**(1), 233–241 (2012).
18. Y. Liu, P. Zhang, Y. Deng, P. Hao, J. Fan, M. Chi, and Y. Wu, "Polymeric microlens array fabricated with PDMS mold-based hot embossing," J. Micromechanics Microengineering **24**, 095028 (2014).
19. S. Kim and S. Kang, "Replication qualities and optical properties of UV-moulded microlens arrays," J. Phys. D Appl. Phys. **36**(20), 2451–2456 (2003).
20. Y. Zhao, C. C. Wang, W. M. Huang, H. Purnawali, and L. An, "Formation of micro protrusive lens arrays atop poly(methyl methacrylate)," Opt. Express **19**(27), 26000–26005 (2011).
21. Y. Zhao, W. M. Huang, and C. C. Wang, "Thermo/chemo-responsive shape memory effect for micro/nano patterning atop polymers," Nanosci. Nanotechnol. Lett. **4**(9), 862–878 (2012).
22. L. Sun, W. M. Huang, Z. Ding, Y. Zhao, C. C. Wang, H. Purnawali, and C. Tang, "Stimulus-responsive shape memory materials," Mater. Des. **33**(2012), 578–640 (2011).
23. A. Y. Yi and L. Li, "Design and fabrication of a microlens array by use of a slow tool servo," Opt. Lett. **30**(13), 1707–1709 (2005).
24. B. McCall and T. S. Tkaczyk, "Fabrication of plastic microlens array for array microscopy by three-dimensional diamond micromilling," Opt. Eng. **49**(10), 103401 (2010).
25. H. M. Leung, G. Zhou, H. Yu, F. S. Chau, and A. S. Kumar, "Diamond turning and soft lithography processes for liquid tunable lenses," J. Micromech. Microeng. **20**(2), 025021 (2010).
26. S. Scheiding, A. Y. Yi, A. Gebhardt, L. Li, S. Risse, R. Eberhardt, and A. Tünnermann, "Freeform manufacturing of a microoptical lens array on a steep curved substrate by use of a voice coil fast tool servo," Opt. Express **19**(24), 23938–23951 (2011).
27. B. McCall and T. S. Tkaczyk, "Rapid fabrication of miniature lens arrays by four-axis single point diamond machining," Opt. Express **21**(3), 3557–3572 (2013).
28. S. Scheiding, A. Y. Yi, A. Gebhardt, R. Loose, L. Li, S. Risse, R. Eberhardt, and A. Tünnermann, "Diamond milling or turning for the fabrication of micro lens arrays: comparing different diamond machining technologies," Proc. SPIE **7927**, 79270N (2011).
29. W.-C. Chen, T.-J. Wu, W.-J. Wu, and G.-D. J. Su, "Fabrication of inkjet-printed SU-8 photoresist microlenses using hydrophilic confinement," J. Micromech. Microeng. **23**(6), 065008 (2013).
30. G. Liu, W. Yu, H. Li, J. Gao, D. Flynn, R. W. Kay, S. Cargill, C. Tonry, M. K. Patel, C. Bailey, and M. P. Y. Desmulliez, "Microstructure formation in a thick polymer by electrostatic-induced lithography," J. Micromech. Microeng. **23**(3), 035018 (2013).
31. B. Jiri Cech, H. Pranov, G. Kofod, M. Matschuk, S. Murthy, and R. Taboryski, "Surface roughness reduction using spray-coated hydrogen silsesquioxane reflow," Appl. Surf. Sci. **280**, 424–430 (2013).
32. J. C. Miñano, M. Hernández, P. Benítez, J. Blen, O. Dross, R. Mohedano, and A. Santamaría, "Free-form integrator array optics," Proc. SPIE **5942**, 59420C (2005).
33. D. Meister and O. World, "Methods for estimating lens thickness," Opt. World **26**(201), 1–5 (1997).
34. Micro.Chem., "MicroSpray™," 2016, <http://www.microchem.com/Prod-Microspray.htm>.
35. ISO 4287., Geometrical Product Specifications (GPS)–Surface texture: Profile method–Terms, definitions and surface texture parameters (1987).

1. Introduction

The fabrication of microlens arrays is exploited more and more nowadays as it is a fundamental component for a wide range of different applications such as optical sensors, biomedical applications, data storage, optical communications, lighting displays, beam homogenizer for color LED system, etc [1–8]. Various techniques for fabricating microlens arrays using direct and/or replication processes have been studied, investigated, demonstrated, and commercially used. Among them are photoresist reflow [9], laser ablation [10,11], etched glass mold [12], grayscale lithography [13,14]. However, most of these methods are either too expensive for mass production or not easily accessible because of the complexity and high cost of the equipment and the processes. Polymer replication processes such as injection molding [15], hot embossing [16–18], and UV molding [19] provides inexpensive mass production solutions to produce precise micro-structured arrays. Lee et. al [15] investigated the injection molding processing condition effects on the replicability of microlens array profile. It was indicated that a packing pressure and a flow rate significantly affects the final

#257628 Received 18 Jan 2016; revised 2 Apr 2016; accepted 11 Apr 2016; published 22 Apr 2016

surface profile of the injection molded product. There are inherent problems using electroplated nickel molds in hot embossing as the pressure distribution between the mold and plastic substrate is not uniform, limiting the embossing area. In UV-molding, shrinkage of the UV-curable material, is limiting the replication quality of UV-molded parts. Zhao et. al [20] proposed a simple two-step process for protrusive lens arrays. The lenslet diameter and height are highly sensitive to applied load to the indents/protrusions and hence, the process is not suitable for the larger sized lenses (i.e., in millimeter and above scale). The surface patterning methods are investigated by the researchers to fabricate 2-D and 3-D patterns utilizing the thermo- and chemo-responsive shape memory effect (SME) in polymeric materials [21]. However, SME is limited for a certain level of shape recovery [22].

Direct fabrication of lens arrays by diamond turning in polymer materials have been demonstrated [23–28] to achieve the high optical surface quality. Although the direct diamond turning process is a one step process, due to process difficulty and expensive tooling, the fabrication process cost could be in the order of USD 100 – 1000 /mm^2. Presently, inkjet printing [29] and electrostatic-induced lithography [30] have been explored for direct fabrication of polymer-based shape controlled lenses. The large dead space between lenslets could be an issue in reducing the optical efficiency considerably. This has been observed in fabricating the microlens arrays considered in this paper through 3D optical printing process making the microlens arrays unsuitable for the application.

Since such direct writing processes are not suitable, we explore a way of improving the surface quality of a CNC machined mold. For any replication technique, the surface quality of the mold considerably affects the quality of the final microstructures and the applicability for optical components. The CNC machining is easy and cheap, but the surface quality is not good enough for optical components. In many cases the CNC machined mold is polished manually, which is tedious, expensive and not applicable for large microlens arrays.

The use of spray-coated hydrogen silsesquioxane coatings to reduce surface roughness was introduced recently [31]. This process requires heating the mold part up to 400 °C in an inert gas atmosphere. Such a high temperature may be challenging to steel types as some of the steel impurities may segregate and cause embrittlement of the steel.

In this paper we describe a novel process, for tool fabrication utilized for injection molding of microlens structures. The process exploits standard CNC milling to make a first rough mold in steel. We introduce a surface treatment by spray coating with photoresist to obtain an optical surface quality required for microlens arrays. The process overcomes the expensive tedious manual polishing or direct diamond turning and provides an easy and inexpensive mold and hence cheap injection molding replication process. The coating process only requires a heat treatment of the mold part up to 175 °C. The fabrication process is demonstrated for production of an ø50 mm double-sided microlens arrays designed for a color mixing LED light engine. The microlens array is designed and optimized in lenslet parameters for large angular acceptance angle and the molding tool is produced from these. Microlens arrays are then injection molded in Polymethyl Methacrylate (PMMA) from both the uncoated rough mold and the photoresist coated mold. The injection molded microlens arrays are characterized through surface measurement by 3D microscopy. The working performance is observed by angular dependent transmission and investigation of light scattering. The implementation of the replicated double sided microlens array in the color mixing LED light engine is described.

2. Method

This section describes the functionality and design aspects of the microlens arrays. The CNC machining of the mold and subsequent procedure for photoresist coating is described. Injection molding of microlens arrays from both the uncoated and coated mold are produced and characterization for surface quality, light scattering and acceptance angle is described.

#257628 Received 18 Jan 2016; revised 2 Apr 2016; accepted 11 Apr 2016; published 22 Apr 2016

2.1 Design of microlens array

We use a double-sided hexagonal patterned convex microlens array, to perform color mixing in a multi-color focusable LED light engine [6,8]. The purpose of the microlens array, called a Kohler integrator [32]], is to combine a large number of quasi-collimated beams from the individual colored LEDs arriving at the microlens array at different angles into a homogenous color mixed beam. Figure 1 illustrates the basic functionality of the microlens array by looking at the ray paths by optical simulation, using Radiant Zemax software, for three collimated beams incident on a single lenslet demonstrated by three different colored beams and the microlens array is simulated here with five lenslets. Figure 1(a) shows the color mixing mechanism for collimated beams at incident angles of 0°, Θ_1° and - Θ_1°, respectively. The three color beams are all focused on the second surface of the same lenslet. The displacements in position of the focal points in the focal plane are dependent on the incidence angles. The maximum incident angle Θ is governed by numerical aperture (NA) of the lenslet through Eq. (1) and is expressed by Eq. (2). From the second surface the three color beams exit the lenslet in the same direction with the same external divergence angle 2Θ.

$$NA = \sin(\theta) = n\frac{D}{2*\sqrt{\left(\frac{D}{2}\right)^2 + f^2}} \cong n\frac{D}{2f} \; when \left(\frac{D}{2}\right)^2 << f^2 \tag{1}$$

$$\therefore \theta = a\sin(NA) \cong a\sin\left(n\frac{D}{2f}\right) \tag{2}$$

Here *D* is the width, and *f* is the focal length of the lenslet and *n* is the refractive index of the lens material, as indicated in Fig. 1(a). Here *r* is the radius of curvature and *t* is the separation distance between two opposite lenslet as seen in Fig. 1(a), respectively. *t* needs to be equal to *f*, so that a collimated beam is focused on the second surface of the lenslet. It is seen that a large divergence angle Θ requires a large numerical aperture, e.g. large *n* and *D* compared to *f*. In the normal operational situation, the incident collimated beams are larger in diameter and hence illuminate a large number of lenslets, and the beams are split into a corresponding number of 'emitters' from each lenslet. Hence the different colored beams incident at different angles on the microlens array, are spatially split into a multitude of emitters with equal divergence and direction, and results in a uniform color mixing of the incoming beams.

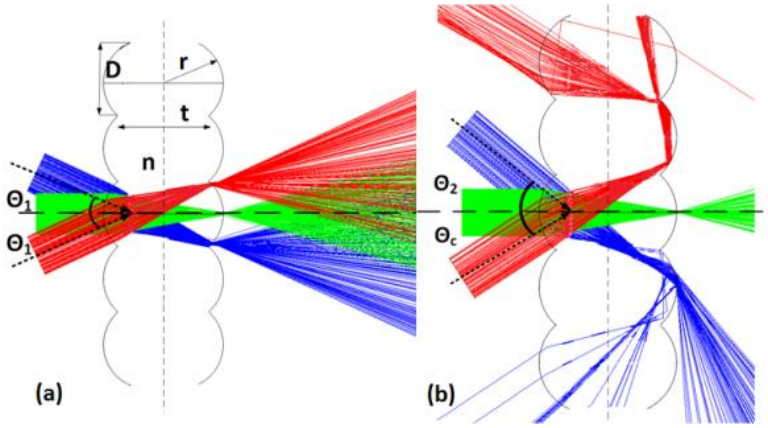

Fig. 1. Basic color mixing functionality of a double-sided, convex microlens array, with incident beams at angles (a) lower than and (b) higher than the acceptance angle.

If the incidence angle is larger than the angle Θ given in Eq. (2), the incident collimated beam is focused and coupled into the neighbor lenslet. This is illustrated in Fig. 1(b) by the

#257628 Received 18 Jan 2016; revised 2 Apr 2016; accepted 11 Apr 2016; published 22 Apr 2016

collimated beam coming from below (red rays). It is seen that if the incident angle exceeds the critical angle at the interface of the second lens surface, the beam is totally internally reflected, where a part of the beam is retuned in the backward direction. In that scenario ideally there will be no transmittance from the second surface of the microlens array. Thus this angle can be called the cutoff angle, $\Theta = \Theta_c$, or equivalently the acceptance angle of the microlens array as within that angle the microlens array allows beams to be transmitted from the second surface of the lenslet [32]]. Figure 1(b) illustrates the case where a collimated beam is incident at an angle larger than the acceptance angle, $\Theta_2 > \Theta_c$ (blue rays). In this case the rays are transmitted in the forward direction from the neighboring lenslet, but at large angles larger than the divergence angle, $\Theta = \Theta_c$. Therefore those rays do not contribute to the effective color mixing within the divergence angle, Θ_c.

According to the above, the transmission of the microlens array would therefore be high for angles lower than Θ_c and close to zero at this angle, and then increase again at larger angles. Figure 1 only illustrates the principle, so in order to get a better idea about the efficiency of the system, we have made a simulation of the transmission through the microlens array using a collimated large beam and varying the incidence angle from 0 to 50°. In order to investigate the output efficiency as a function of exit angle the simulation is done for a detector that measures the light transmitted within an exit cone of varying angle. Figure 2 shows the transmission efficiency of the microlens array for the varying incident angles and for varying exit cone half angles. It can be seen that for incidence angles from 0 to 30°, more than 90% of the light is transmitted when the exit cone half angle is larger than 40°. This corresponds to the case in Fig. 1(a) where the beams are incident at angles lower than the acceptance angle and where the exit cone covers the acceptance angle. For incidence angles around 40° almost no light is transmitted within the exit cone of 40°. This corresponds to the case where the incidence angle is close to the acceptance angle as illustrated in Fig. 1(b) by the red rays. The top part of the graph in Fig. 2 corresponds to a large exit cone angle of around 80° e.g. collecting all the transmitted light. Here efficiency higher than 40% is observed for incidence angles around 45°, corresponding to the case in Fig. 1(b) (blue rays), however, this transmitted light does not contribute to the mixed light within the divergence angle.

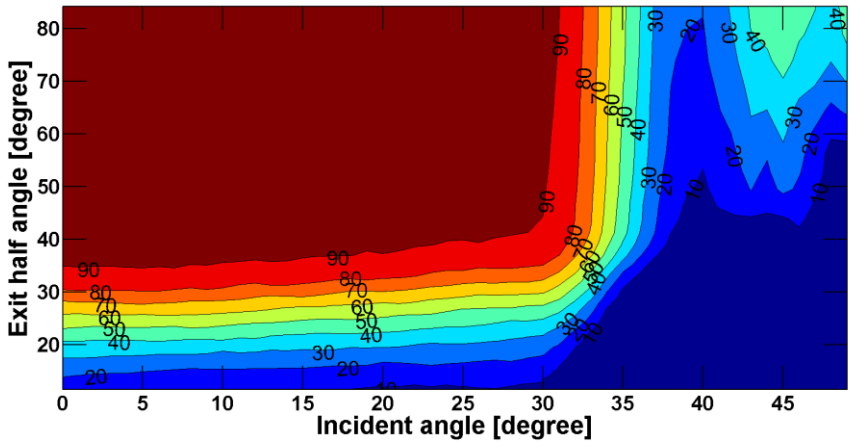

Fig. 2. Simulated transmission efficiency [%] of microlens array as a function of incident angle of collimated beam. Efficiency is simulated for varying exit cone angles.

To achieve high optical efficiency of the light output from the light engine, the acceptance angle of the microlens array needs to be optimized. Therefore the microlens array for the LED light engine [6] has been designed to have a large acceptance angle. It is seen from Eq. (2) that a large divergence angle Θ requires a large numerical aperture *NA*, e.g. large *n* and *D* compared to *f*. However, the overall transmittance decreases linearly with the increase of *n* of

#257628 Received 18 Jan 2016; revised 2 Apr 2016; accepted 11 Apr 2016; published 22 Apr 2016

the material due to Fresnel loss, i.e. reflections at surface air interfaces. Thus there would be a tradeoff between transmittance and acceptance angle. For injection molding the choices of materials most widely used are Poly Carbonate (PC) or PMMA. Although the higher *n* of PC yields a larger acceptance angle than using PMMA, the transmittance is lower. A simulation of the transmittance of the microlens array for the two different materials have been performed using an incident cone of light integrating over all angles within the cone angle and a large exit cone angle. Figure 3 shows this simulated transmittance as a function of the incident cone angle for PC and PMMA respectively. It shows that the transmittance of the PMMA microlens array is higher than the one using PC for all incidence cone angles. The transmission through PMMA microlens is ~3% higher than for PC at almost perpendicular incidence. PMMA also has ~5% larger efficiency at high incident cone angle of 50°. In our application we prioritize the transmittance and chose PMMA as the material for the microlens fabrication.

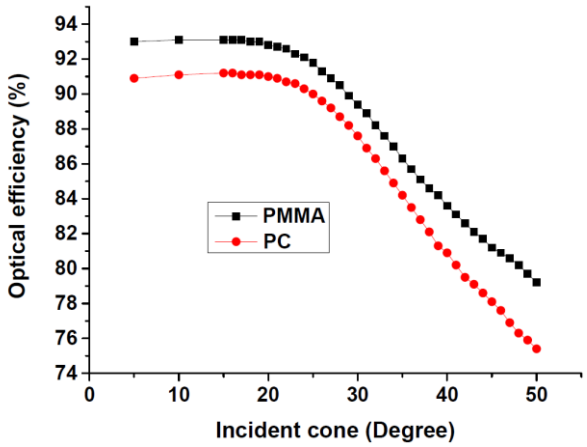

Fig. 3. Simulation of transmission efficiency of microlens array as a function of incidence cone for the two different materials, PMMA and PC.

In order to enhance the optical efficiency in our LED system, the high NA value is also required. The lenslets are spherical with a radius of curvature, *r*, and the diameter *D* of the single lenslet varies with the sag [33]. A thorough study was done on different lenslet parameters targeting the enhancement of the acceptance angle and finally the design was optimized by simulation. Table 1 lists the designed lens parameters used for the microlens array fabrication after optimizing the parameters.

Table 1. Lens parameters for fabricated microlens.

Material	Microlens array size [mm]	Total thickness (double sided) [mm]	curvature for lenslet [mm]	Sag [mm]	Lenslet width[mm]	Focal length (mm)	Acceptance angle [°]
PMMA	65	2.1	0.85	0.55	1.45	1.4	82

2.2 Fabrication process

In this section the fabrication of the double sided microlens array is described, from the CNC fabrication of mold, the coating procedure with photoresist and the injection molding. The CNC machine was loaded by the computer generated drawing file, made by SolidWorks software, which holds the design optimized lens parameters information [Table 1] about the microlens array. After that the CNC machine inscribes the loaded microlens array structures on a steel block as shown in Fig. 4, by using a standard spherical milling tool with a radius of 0.85mm. Similar kind of block needs to make which has been held on top of the bottom block. The alignment of the two blocks requires precision so that the positions of the microlens structures in both blocks can overlap to each other. As shown in the figure, there is

#257628 Received 18 Jan 2016; revised 2 Apr 2016; accepted 11 Apr 2016; published 22 Apr 2016

an inlet for injection molding at the edge of the microlens structure. The accuracy of the CNC machine is +/–50 µm.

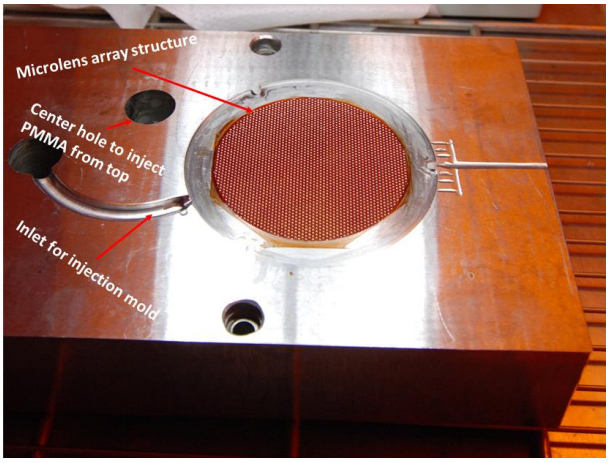

Fig. 4. One side of mold tool for ø65mm microlens array in a steel block.

The surface roughness of the steel mold can be reduced by photoresist coating. Spin coating is not possible for this application and in order to overcome this problem we have used MicroSpray™ photoresist [34]. Microspray is a positive acting, aerosol novolak resist and suits our application. It is cost effective, easy to use and spray eliminated the irregularities and peak – valley variations on the surface of the mold according to our requirements. For best use we placed the Microspray at room temperature (~20 °C) for an hour prior to use. Before applying, the Microspray needs to be shaken strongly for 10 times and needs to wait for 5 minutes to remove any air bubbles. Before coating, the steel mold needs to be cleaned by metal cleaner. After applying the coating, the mold requires to be soft and hard baked. The thermal crosslinking achieved through the hard baking makes the photoresist robust during the injection molding. The block diagram in Fig. 5 shows the entire coating process.

#257628 Received 18 Jan 2016; revised 2 Apr 2016; accepted 11 Apr 2016; published 22 Apr 2016

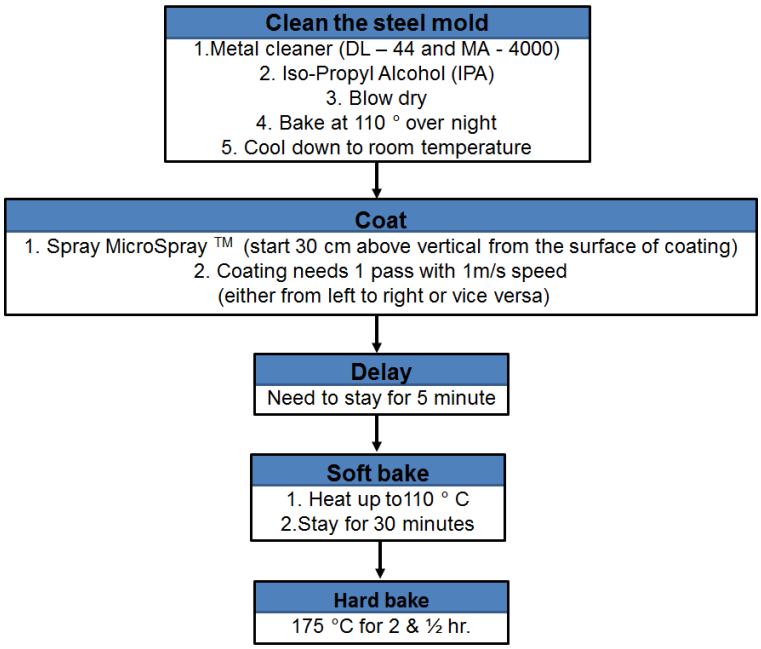

Fig. 5. Photoresist process sequence.

The coating thickness was inspected through Dektak measurements on a separate sample, to be from 10 to 14 μm, where the standard deviation of the thickness is ~2.6%. The polymer PMMA is the best candidate to use as the material for the microlens array for our application as explained above. It has also the advantages of the material properties especially the versatile polymeric material is well suited for imaging / non-imaging application.

The mold was installed in a standard injection molding machine, in which the second steel block was aligned by dowel pins with 50 micron accuracy and placed on the top of the first block, and PMMA was injected through the center hole of the top block. PMMA was then channelized through the inlet [Fig. 4]. Afterwards a heavy pressure of 2500 bar was applied to the polymer melt. The process cycle of the microlens array is ~20 sec. Melting temperature of PMMA was 210 °C and the mold temperature was 70 °C. Injection molded microlens arrays were produced in the first iteration using the uncoated rough mold. After photoresist coating of both steel molds (top and bottom one) a second iteration of injection molding of microlens arrays was performed. The injection molding was performed by the Danish company JJ Kühn. About 100 microlens arrays were produced without any sign of wear off the photoresist, and without any measurable differences between the item 1 and 100.

2.3 Characterization of the microlens array

After fabrication of the microlens array we have characterized the surface quality looking at pre and after coating process result. We have measured lens parameters of the fabricated lenslets by analyzing the arrays under 3D confocal and interferometric microscopy (Sensofar Plu-neox). The analytical results for surface quality and the quantitative measurement on lens parameters are shown in the *Result and discussion* section.

The optical performance with regard to the application was investigated by measuring the angular dependence of the transmission and investigating the light scattering effect. Figure 6 illustrates the setup for simulating the transmitted light as a function of incident cone and different exit cones. It also describes the transmission measurement, where a collimated white light beam with a beam diameter of 10 mm from a fiber coupled source (Ocean Optics HL 2000) was used. The incidence angle was varied over the interval ± 45°. The transmitted light was measured as a function of incidence angle using a 6 inch integrating sphere as collection

#257628 Received 18 Jan 2016; revised 2 Apr 2016; accepted 11 Apr 2016; published 22 Apr 2016

optics. The microlens array was mounted at the 1 inch diameter port opening and the exit cone half angle is nearly 90°, which corresponds to the top part of the simulation results shown in Fig. 2. The results from the measurement are shown in below. The transmitted light was measured using a spectrometer (QE 65000) fiber coupled to the sphere. Further the light scattering from the surface of the microlens array is investigated by looking at the reflected laser light of a single lenslet.

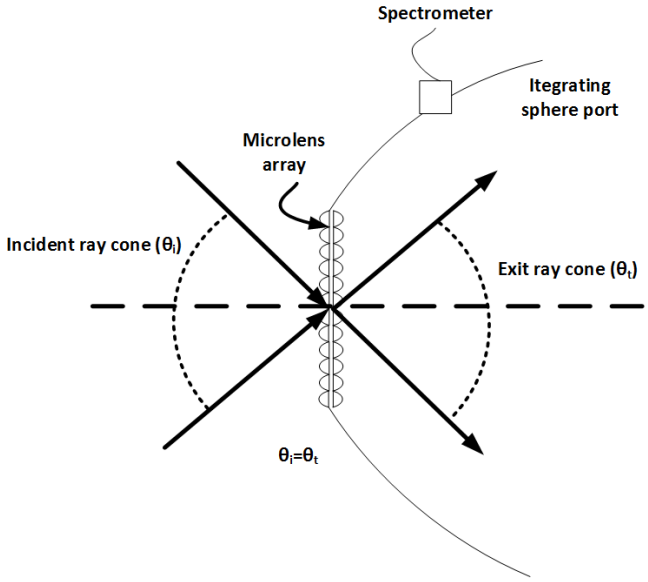

Fig. 6. Sketch illustrating the simulation and experimental set-up for measuring angular transmission and acceptance angle of the microlens array.

3. Results and discussion

In this section the properties of the injection molded samples from the uncoated and coated mold tool is compared. The confocal microscopy measurement was done using the objective of Nikon 50x with NA 0.95. The 3D images have been taken for 5 consecutive lenslets by the method of stitching 3x3 images with the condition of 25% overlap. From each of the two microlens arrays 5 individual lenses have been analyzed. The diameter of the lens array including the outer ring is 85 mm as shown in Fig. 7(a). The position of the central lens was 39 mm from the edge of the perimeter of the outer ring and the five consecutive lenslets were taken for the measurements from that region. The diameter of the hexagonal lenses is measured as edge to edge distance which is measured by Fourier transform of the image (20x microscope images) to identify a unit cell or lenslet. Thus the whole image is used for the measurement [seen in Fig. 7(b)]. The total height of the lens is measured from the stitched image (1x8 50x) as seen in Fig. 7(c) where the center and the edge of the single lenslet is visible. The vertical distance from the edge to the center of the lenslet gives the height. The radius of curvature is measured for each lens by fitting a sphere to the 3D surface. The aberration from this sphere is also investigated as a 3D image. The roughness of the surface is also measured after suitable waviness filtration. Table 2 summarizes the measured results for the lens parameters. The standard deviation between all measurements for radius of curvature is 35µm. Thus it shows the repeatability and reproducibility of the fabrication process within ± 50 µm accuracy. The values corresponding to uncoated and coated are equal within the uncertainties and shows that the coating process does not affect the lenslet parameters.

#257628 Received 18 Jan 2016; revised 2 Apr 2016; accepted 11 Apr 2016; published 22 Apr 2016

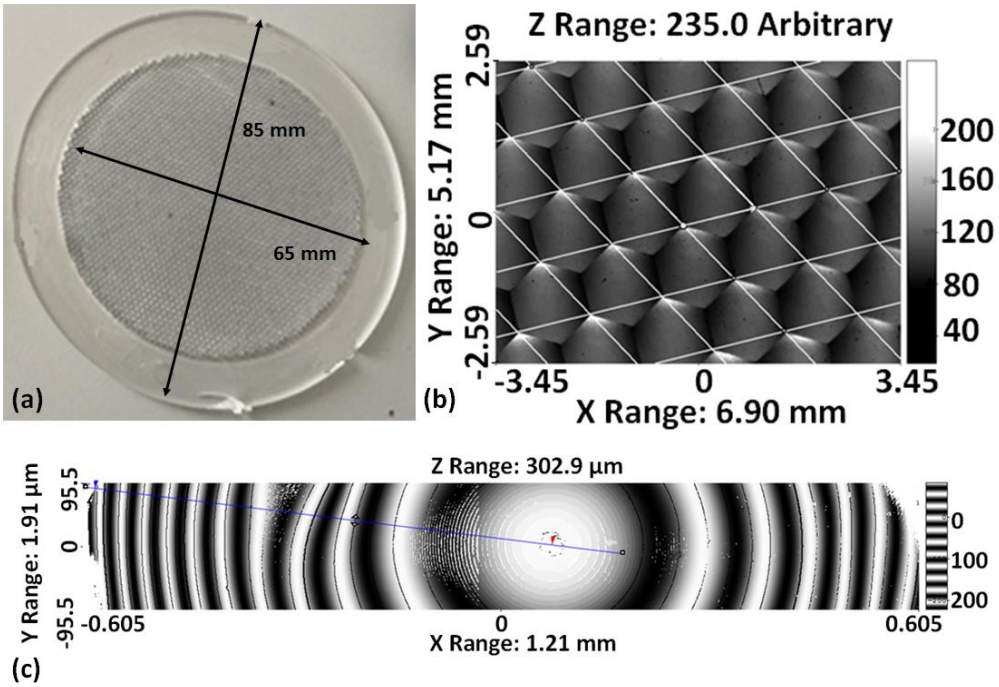

Fig. 7. (a) Photo of the injection molded sample; (b) Magnified view of the selected portion of the five lenslets for measuring the lens width; (c) Magnified single lenslet for height measurement.

Table 2. Measure single lens parameters by 3D microscopy

Microlens array type	Radius of curvature for lenslet [mm]	Sag [mm]	lenslet width [mm]
Uncoated	0.863 ± 0.040	0.503 ± 0.001	1.457 ± 0.005
Coated	0.869 ± 0.035	0.492 ± 0.001	1.46 ± 0.005

We have investigated the surface quality of the lenslet through surface topography measurements. Figure 8 compares the images of the top surfaces of lenslet from the uncoated (left) and coated (right) mold, respectively, after fitting with sphere of radius 846.1 µm. The surface roughness is calculated by measuring R_a, R_q and R_z [35] which are shown in Table 3. There is some cast defect also at the edge of the perimeter of the array. However, those defects did not influence the light path. It is observed that the photoresist coating of the mold improves the surface roughness of the injection molded microlens arrays, in reducing the R_a, R_q and R_z by factors of 2, 2.5 and 2.6 respectively. It is seen from the cross-sections [Fig. 8(c) and 8(d)] that the maximum variation is reduced from 1.2 µm to 0.2 µm for these specific scans.

#257628 Received 18 Jan 2016; revised 2 Apr 2016; accepted 11 Apr 2016; published 22 Apr 2016

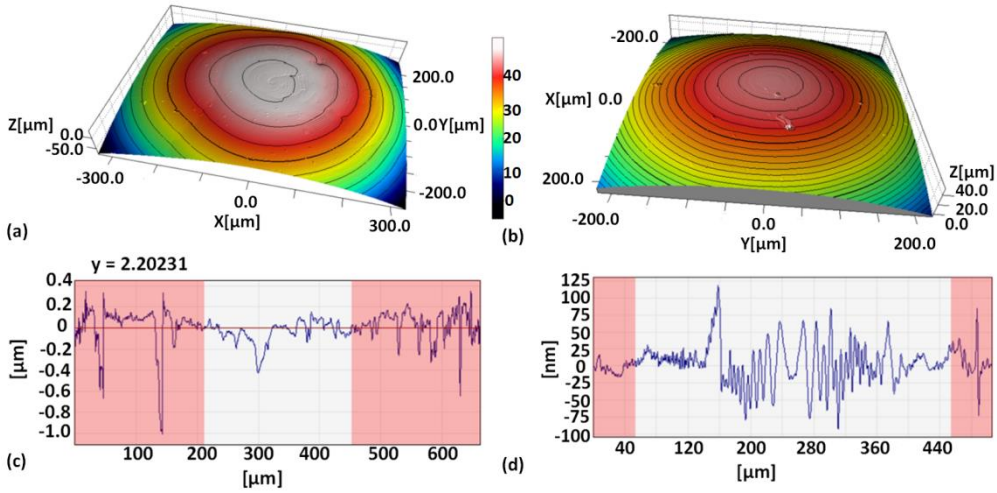

Fig. 8. Topography image with height contours for each 2 µm in the z-direction for microlens lenslet from (a) (shown 600 x 600 µm^2 area) uncoated and (b) (shown 400 x 400 µm^2 area) coated mold and corresponding surface variation along cross section in (c) and (d) respectively.

Table 3. Roughness Measurement According to ISO 4287:1997 [35].

Microlens array type	Ra*[a] [nm]	Rq*[b] [nm]	Rz*[c] [nm]
Uncoated	75 ± 29	110 ± 56	441 ± 194
coated	38 ± 1	42 ± 2	173 ± 26

* [a]R_a: arithmetic average of absolute value for surface roughness, * [b]R_q: root mean square (rms) average of the roughness profile ordinates, * [c]R_z: the mean roughness depth which is the arithmetic mean value of the single roughness depths of consecutive sampling lengths.

The working performance of the injection molded microlens array from the coated mold has been investigated through measurement of the angular transmission, Fig. 9 shows the measured transmission as a function of incidence angle and the corresponding simulation is shown as well. This is used to determine the acceptance angle of the microlens array Fig. 9 shows the corresponding results for another microlens array with D = 1.2 mm used in the first prototype of the LED light engine. The acceptance angle for this is 37°. For the optimized design of the microlens array produced in this work, the NA has been increased by increasing the width D to a value of 1.45 mm. The measurement for this in Fig. 9, shows a maximum transmission of ~92% which is almost constant within ± 40°, hence an acceptance angle of 40°. The refractive index of PMMA is 1.489. Thus the Fresnel reflection loss per interface for 2.1 mm microlens array is ~3.9% and thus transmission from the array was ~92%. Again the calculated acceptance angle according to Eq. (2) is ~41°. Hence, there is good correspondence between simulation and measurements on the produced microlens array. Due to machine accuracy in lens parameters; there is a discrepancy of ~2° in acceptance angle between the simulation and the experiment. The increasing measured and simulated efficiency at angle larger than ± 40° corresponds to the coupling of light through the neighbor lenslets, illustrated in Fig. 1(b).

#257628 Received 18 Jan 2016; revised 2 Apr 2016; accepted 11 Apr 2016; published 22 Apr 2016

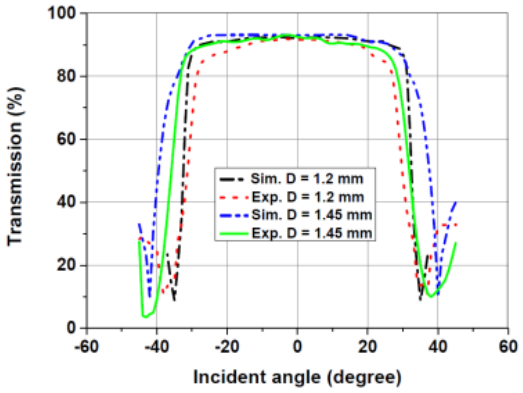

Fig. 9. Comparison of microlens array by both simulation (Sim.) and experiment (Exp.) respectively.

Figure 10 shows the results of the visual and light scattering investigation of the surface quality. The investigation is on a single lenslet, where the images to the left shows photos of the top surface taken by optical microscope and the images on the right are photos of the reflected light when a lenslet is illuminated by a He-Ne laser beam. The images in Fig. 10(a) are for the injection molded microlens array from the uncoated mold. Irregularities are seen on the microscope image and the reflected He-Ne laser beam is strongly distorted and scattered. This surface quality is not good enough for the microlens application. The microlens array produced from the photoresist coated mold, has a much improved surface quality as seen in Fig. 10(b), there are much fewer irregularities in the microscope image and the reflected He-Ne laser beam is nearly undistorted and less scattered light has been observed. This surface quality is applicable for the LED light engine application and a 5% increase of the efficiency of this was observed when using the microlens array form the coated mold compared to the one from the uncoated mold.

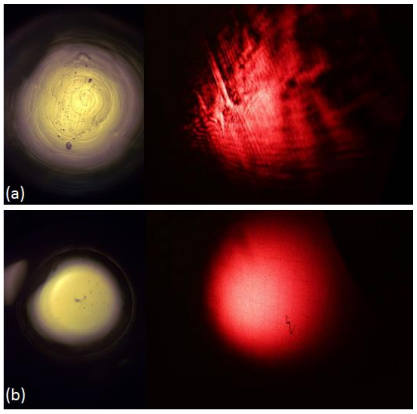

Fig. 10. Optical microscopic images of a single lenslet (left side) and photo of transmitted He-Ne laser beam from a single lenslet (right side) in injection molded microlens array from the (a) uncoated mold and (b) photoresist coated mold.

4. Conclusion

A novel tool fabricating process is reported which allows cheap and fast machining of molding tools for injection molding. The process is based on simple CNC machining of a steel block as a rough tool and subsequent spray coating of the tool with photoresist. This achieves the desired optical surface quality required for the microstructures fabrication. The process is demonstrated by making a double sided hexagonal patterned microlens array for

#257628 Received 18 Jan 2016; revised 2 Apr 2016; accepted 11 Apr 2016; published 22 Apr 2016

the application of beam homogenization in the LED light engine. Injection molded samples were produced in PMMA from both the uncoated and coated mold tool. Experimental investigations of the lenslet parameters and surface roughness were carried out using 3D confocal and interferometric microscopy. The lenslet parameters corresponding to uncoated and coated are found to be equal within the measurement uncertainties and shows that the coating process does not affect the lenslet parameters. The surface roughness was investigated by measuring the quantities of R_a, R_q and R_z for the both uncoated and coated microlens array. The coating with photoresist of the mold improves the surface roughness of the injection molded microlens array reducing R_a, R_q and R_z by factor of 2, 2.5 and 2.6 respectively. The improvement of surface roughness was also evident by investigating the light scattering effect from the top surface of the lenslet. Initially, the lenslet width was optimized in order to maximize the acceptance angle which enhances the optical efficiency of the LED light engine.

The acceptance angle of the injection molded microlens array from the coated mold was measured to be ~40° in accordance with the simulations.

Acknowledgment

We would like to thank the Danish Council for Technology and Innovation under the Innovation Consortium LICQOP, grant #2416669 and The Danish National Advanced Technology Foundation under the V8 light engine project (037-2011-3) for their financial support. We would also like to acknowledge the help from Jan Kühn from the company JJ Kühn A/S for fabrication of the steel mold and injection molding of the sample. We would like to acknowledge Stela Canulescu and Maria Louisa Rosenberg Welling from Technical University of Denmark for technical and editorial support.

#257628 Received 18 Jan 2016; revised 2 Apr 2016; accepted 11 Apr 2016; published 22 Apr 2016